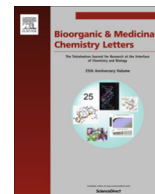




Contents lists available at ScienceDirect

Bioorganic & Medicinal Chemistry Letters

journal homepage: www.elsevier.com/locate/bmcl

Discovery and crystallography of bicyclic arylaminoazines as potent inhibitors of HIV-1 reverse transcriptase

Won-Gil Lee^a, Kathleen M. Frey^b, Ricardo Gallardo-Macias^a, Krasimir A. Spasov^b, Albert H. Chan^b, Karen S. Anderson^{b,*}, William L. Jorgensen^{a,*}^a Department of Chemistry, Yale University, New Haven, CT 06520-8107, USA^b Department of Pharmacology, Yale University School of Medicine, New Haven, CT 06520-8066, USA

ARTICLE INFO

Article history:

Received 17 June 2015

Accepted 22 June 2015

Available online xxx

Keywords:

HIV-1 reverse transcriptase

NNRTI

Structure-based drug design

Protein crystallography

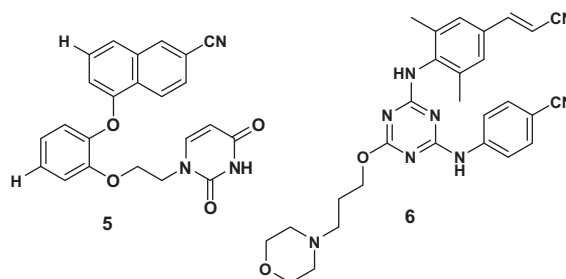
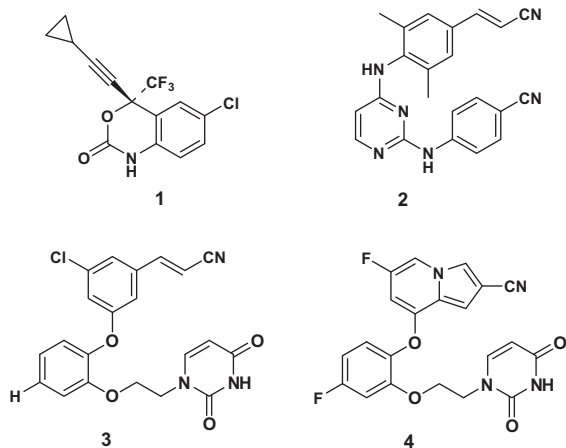
Drug solubility

ABSTRACT

Non-nucleoside inhibitors of HIV-1 reverse transcriptase (HIV-RT) are reported that incorporate a 7-indolizylamino or 2-naphthylamino substituent on a pyrimidine or 1,3,5-triazine core. The most potent compounds show below 10 nanomolar activity towards wild-type HIV-1 and variants bearing Tyr181Cys and Lys103Asn/Tyr181Cys resistance mutations. The compounds also feature good aqueous solubility. Crystal structures for two complexes enhance the analysis of the structure–activity data.

© 2015 Published by Elsevier Ltd.

Non-nucleoside inhibitors of HIV-1 reverse transcriptase (NNRTIs) are an essential element of anti-HIV therapy.¹ Efavirenz (**1**) and rilpivirine (**2**) are components of the one-a-day triple-combination therapies Atripla and Complera.² In spite of their success, there is a need for continued development of NNRTIs in view of the rapid mutation of the virus, varying resistance and side effect profiles, and evolving risks of long-term treatment.^{3–5}



To this end, we have explored multiple series of NNRTIs. The work is challenging owing to the needs for potency towards wild-type HIV-1 and multiple commonly observed viral variants, and for good pharmacological properties. Dosage (600 mg/day), resistance, and CNS side effects are problematic for efavirenz, while poor solubility and virologic failure are issues with rilpivirine.^{2,4} Significant headway in potency was made for our series with the discovery of catechol diethers.⁶ Assays tested activity against wild-type HIV-1 and the most common clinically observed viral variants, which contain Tyr181Cys (Y181C) and Lys103Asn (K103N) point mutations in the reverse transcriptase enzyme. EC₅₀ values as low as 0.055 nM were obtained for inhibition of viral replication in human T-cells infected with the wild-type virus.⁶ Overall, **3** is among the best examples with EC₅₀ values of 0.31, 46, and 24 nM towards wild-type HIV-1, and virus containing the Y181C mutation and the particularly challenging K103N/Y181C double variant. Though the

* Corresponding authors.

E-mail addresses: karen.anderson@yale.edu (K.S. Anderson), william.jorgensen@yale.edu (W.L. Jorgensen).

activity of **3** towards the variants is less than for **1** or **2**, the compound has remarkable aqueous solubility and relatively low toxicity towards human T-cells (CC_{50} = 18 μ M), as summarized in Table 1.

However, **3** like rilpivirine incorporates a cyanovinyl group, which is rarely found in drugs owing to concerns for Michael additions that might lead to undesirable covalent modifications of proteins or nucleic acids.⁷ Thus, less reactive alternatives were pursued by incorporating the cyanovinyl fragment into a 6:5 or 6:6 bicyclic ring system.^{7,8} Resultant notable examples include **4** and **5**. The indolizine **4** shows excellent potency towards the wild-type virus and the double variant, low cytotoxicity, and good aqueous solubility; however, it and the other 6:5 bicyclics are oddly much less active towards the Y181C single variant.⁷ This problem was largely overcome with 2-naphthyl catechol diethers.⁸ For example, **5** has all three EC_{50} values below 20 nM and shows no cytotoxicity, but its solubility is only 4.3 μ g/mL, which is at the bottom of the range normally observed for oral drugs.⁹

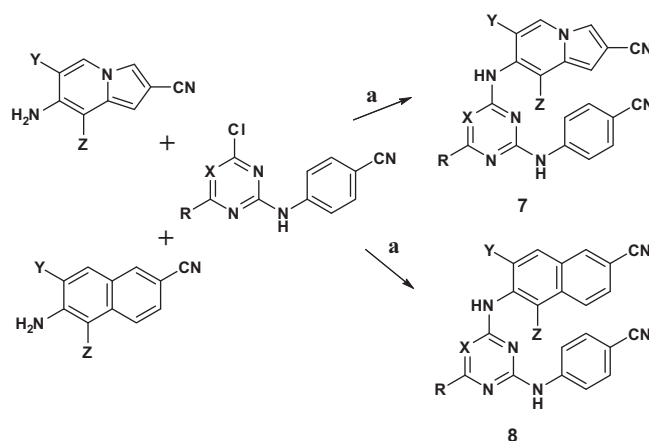
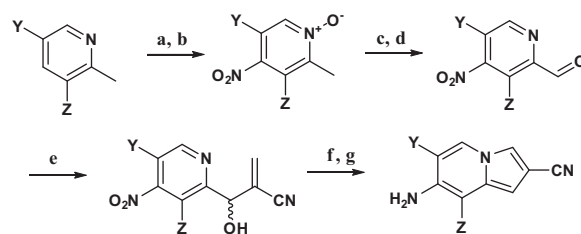
Simultaneously, analysis of crystal structures and molecular modeling led us to realize that the solubility of anilinyllazines such as **2** could be enhanced without unacceptable loss of potency by judicious placement of a polar substituent that would project into the entrance channel of the NNRTI binding site.¹⁰ This led to discovery of **6**, a morpholinylpropoxytriazinyl analogue of **2**, which has excellent potency and greatly improved solubility (14.2 μ g/mL).¹¹ Nevertheless, further efforts were deemed desirable to replace the cyanovinyl group in **6** and also to seek additional gains for potency and solubility. As described here, success was obtained by combining the 6:5 and 6:6 bicyclic notion with anilinyll pyrimidine or triazine cores in **7** and **8**.

Compounds listed in Table 2 were prepared as summarized in Schemes 1–3. The final products come from Pd-catalyzed amination of chloroazines (Scheme 1).¹¹ The morpholinylpropoxy analogues were derived from the **7** and **8** triazinyl chlorides (X = N, R = Cl) by reaction with 3-morpholinopropan-1-ol and NaH in 1,4-dioxane for 16 h at 90 °C. The requisite 7-aminoindolizines were derived from substituted pyridines, which after oxidation, and nitration, underwent a Baylis–Hillman reaction, cyclization, and reduction to yield the desired intermediates.⁷ For the 2-aminonaphthalenes, acetals **9** were prepared by alkylation of dimethyl 2-(2,2-diethoxyethyl)malonate with benzyl bromides. Cyclization to the methyl naphthoate was followed by conversion of the ester progressively to the aldehyde and nitrile. Finally, the 2-amino group was introduced by Pd-catalyzed reaction of the bromides with *t*-butyl carbamate, followed by acid-catalyzed removal of the Boc group.

In the same manner as in previous reports,^{6–8,10,11} activities against the IIB strain of HIV-1 were measured using MT-2 human T-cells; EC_{50} values are obtained as the dose required to achieve 50% protection of the infected cells by the MTT colorimetric

Table 2Anti-HIV-1 activities (EC_{50}) and cytotoxicity (CC_{50})^a

Compd	R ^b	X	Y	Z	EC_{50} WT	EC_{50} Y181C	EC_{50} K103N/Y181C	CC_{50}
7a	H	CH	H	H	200	NA	NA	>100,000
7b	H	CH	Me	H	30	510	6200	72,000
7c	H	CH	H	Me	1.4	26	170	>100,000
7d	H	CH	Me	Me	1.0	0.57	39	10,100
7e	H	CH	F	H	200	1600	4600	76,000
7f	H	CH	F	F	1.4	98	NA	1000
7g	H	N	Me	Me	0.52	7.1	32	16,000
7h	Cl	N	Me	Me	14000	NA	NA	38,000
7i	H	N	F	F	2.7	230	2200	20,000
7j	Mo	N	H	Me	1900	NA	NA	10,000
8a	H	CH	H	H	24	170	520	>100,000
8b	H	CH	H	Me	7.0	8.5	130	>100,000
8c	H	CH	Me	Me	2.9	2.2	6.9	7800
8d	H	CH	H	F	6.0	70	790	45,000
8e	H	CH	F	F	1.8	6.0	50	4800
8f	H	N	Me	Me	1.1	1.3	7.0	9500
8g	Cl	N	Me	Me	2.3	41	67	7500
8h	H	N	F	F	1.2	7.0	65	>100,000
8i	Mo	N	H	H	120	NA	150	1200
8j	Mo	N	H	Me	21	58	98	5900
8k	Mo	N	H	F	36	160	180	3800
8l	Mo	N	Me	Me	17	36	16	17,000

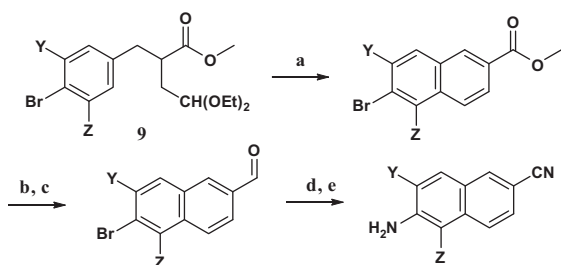
^a EC_{50} and CC_{50} in nM from infected T-cell assays. NA = not active (EC_{50} > CC_{50}).^b Mo = N-morpholinylpropoxy as in **6**.**Scheme 1.** Synthesis of **7** and **8** where X = CH, N; R = H, Cl; Y, Z = H, F, Me. Reagents and conditions: (a) BINAP, $Pd_2(dba)_3$, 1,4-dioxane, 90 °C, 12–24 h.**Scheme 2.** Synthesis of substituted indolizines. Reagents and conditions: (a) *m*-CPBA, $CHCl_3$, rt, 18 h; (b) HNO_3 , H_2SO_4 , 95 °C, 4–16 h; (c) (i) Ac_2O , 110 °C, 4 h; (ii) HCl , 70 °C, 3 h; (d) SeO_2 , 1,4-dioxane, 90 °C, 16 h; (e) acrylonitrile, DABCO, neat, rt, 1.5 h; (f) Ac_2O , 100–135 °C, o/n; (g) Pd/C , H_2 , MeOH, rt, 12 h.

method. Simultaneously, CC_{50} values for inhibition of MT-2 cell growth by 50% are obtained. The analyses used triplicate samples at each concentration. The identity of all assayed compounds was confirmed by 1H and ^{13}C NMR and high-resolution mass spectrometry; purity was >95% as judged by high-performance liquid

Table 1
Anti-HIV-1 activities (EC_{50}), cytotoxicity (CC_{50}), and aqueous solubility^a

Compd	EC_{50} WT	EC_{50} Y181C	EC_{50} K103N/Y181C	CC_{50}	S (μ g/mL)
1	2.0	10	30	15,000	68.0
2	0.67	0.65	2.0	8000	0.02 ^b
3	0.31	46	24	18,000	510
4	0.40	250	10	50,000	43.8
5	0.53	19	15	>100,000	4.3
6	1.2	12	1.3	4500	14.2
7d	1.0	0.57	39	10,100	8.2
7g	0.52	7.1	32	16,000	33.1
8c	2.9	2.2	6.9	7800	12.2
8f	1.1	1.3	7.0	9500	28.7

^a EC_{50} and CC_{50} in nM from infected T-cell assays. Data for **1**–**6** from Refs. 6–8.^b Ref. 15.



Scheme 3. Synthesis of substituted naphthalenes. Reagents and conditions: (a) aq 80% H_2SO_4 , MeOH, DDQ, 0 °C to rt, 1 h; (b) DIBAL, THF, –78 °C to rt, o/n; (c) PCC, DCM, rt, 2 h; (d) NaN_3 , TFOH, ACN, rt, 1 h; (e) (i) *t*-butyl carbamate, $\text{Pd}_2(\text{dba})_3 \cdot \text{CHCl}_3$, xantphos, Cs_2CO_3 , toluene, 100 °C, 16 h; (ii) 2 N HCl, 1,4-dioxane, 60 °C, 2 h.

chromatography. Aqueous solubilities were also measured as previously described using a shake-flask procedure in Britton–Robinson buffer at pH 6.5 and 25 °C.^{10–12} The supernatant was collected using a 0.2 μm Pall Life Sciences Acrodisc syringe filter, and analyzed by UV–vis spectrophotometry (Agilent 8453).

Interpretation of the structure–activity data was facilitated by obtaining crystal structures of several compounds in complex with HIV-1 RT. Following previously reported procedures,^{7,8,10,11,13} crystals were obtained with recombinant RT enzyme that diffracted to 2.6–2.8 Å on beamlines at the Brookhaven NSLS or Argonne APS.¹⁴ For **7g** (Fig. 1), the indolizine ring is positioned in the NNRTI binding site as expected from the earlier studies to make aryl–aryl interactions with Tyr181, Tyr188, and Trp229. The plane of the indolizine ring is perpendicular to the anilinyltriazine fragment and there is a characteristic hydrogen bond between the anilinylnh and the backbone carbonyl group of Lys 101 (2.59 Å).^{10,11,13,15} In this structure, Tyr181 and Tyr188 are in the ‘up–up’ conformation, that is, typical for anilinyllazines, and Glu138 and Lys101 are forming a salt-bridge. A rendering of the crystal structure of **8f** with HIV-1 RT, which illustrates the orientation of the substituted naphthalene ring system and the cluster of aromatic residues, is provided in Figure 2.

Turning to the data in Table 2, the parent indolizinyln pyrimidine **7a** is a modest inhibitor of the wild-type virus (200 nM) and is not active towards the two variants. Progressive methylation at the 6- and 8-positions (**7b–7d**) dramatically enhances the potency.

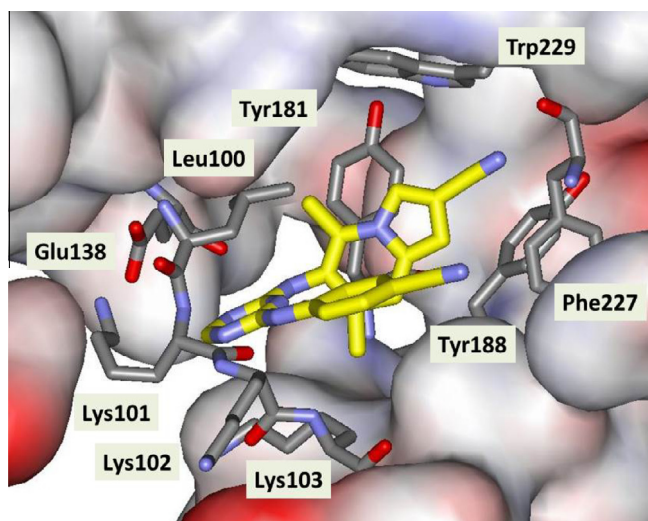


Figure 1. Rendering from the crystal structure of **7g** bound to WT HIV-RT. Some residues are omitted for clarity. Coordinates have been deposited in the PDB as structure 5C24.

The same pattern is found for fluorination with **7e** and **7f**, but to a lesser extent. This observation is readily attributed to the buttressing by the added groups that forces the indolizine ring to be perpendicular to the azine ring, yielding better preorganization for binding (Fig. 1). The effects are larger for the bulkier methyl groups. **7g**, the triazine analogue of **7d**, is also impressive with EC_{50} values of 0.52, 7.1, and 32 nM towards the wild-type virus and the two variants. Less potency is again found with the difluoro analogue **7i**, and a chlorine (**7h**) or a morpholinylpropoxy group (**7j**) at the 6-position of the triazine ring are not well tolerated owing to steric interference with the Lys101–Glu138 salt bridge.

The parent naphthyl pyrimidine **8a** is significantly more potent than the corresponding indolizine **7a**. This appears to be due to improved aryl–aryl contacts with Tyr181 and Trp229 (Figs. 1 and 2). Methylation or fluorination at the 1- and 3-positions again provides significant gains in inhibitory activity (**8b–8e**). The dimethyl pyrimidine and triazine analogues **8c** and **8f** are the best new compounds for potency with sub-10 nM results for all three viral forms. Addition of a chlorine at the 6-position of the triazine diminishes activity, though not as much as in the indolizine series. The difluoro analogue **8h** shows no cytotoxicity, but it performs less well than **8f** for the HIV-1 variants. A methyl group is expected to better fill the space vacated upon the Tyr181Cys exchange than a fluorine. Finally, the morpholinylpropoxy analogue **8i** is interesting; the added substituent is much better tolerated than for **7j**. An explanation is not obvious from the crystal structures as C6 of the triazine is 3.61 and 4.06 Å away from the closest oxygen of Glu138 and ammonium nitrogen of Lys101 for **7g** and 3.29 and 4.14 Å for **8f**.

Aqueous solubilities for the most potent new compounds were determined and are compared with the previously reported values for **1–6** in Table 1. The results for the triazines **7g** and **8f**, 33 and 29 $\mu\text{g/mL}$, are well within the normal range observed for oral drugs.⁹ The corresponding pyrimidines, **7d** and **8c**, are 2–4 fold less soluble than the triazines. The pyrimidines are also somewhat more cytotoxic than the triazines (lower CC_{50} values). The profoundly low solubility of rilpivirine (0.02 $\mu\text{g/mL}$)¹⁵ is striking. The much higher solubility of the indolizines was expected,⁷ but the similarly higher solubility of the naphthalene analogues is surprising;⁸ it must reflect subtleties in crystal packing.

In summary, exploration of alternatives for the cyanovinyl group in catechol diethers like **3**, led to indolizine and naphthalene containing alternatives including **4** and **5**.^{7,8} Attempts at improving the solubility of our own anilinyllazines¹⁰ as well as rilpivirine led to **6**.¹¹ Merger of these series has now brought us to **7** and **8**. The

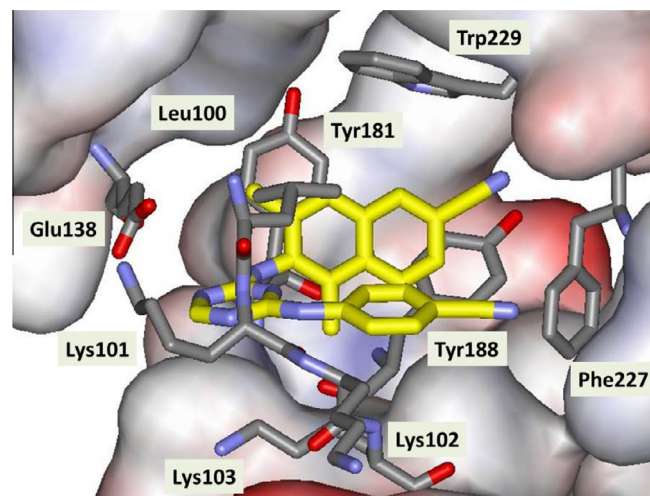


Figure 2. Rendering from the 5C25 crystal structure of **8f** bound to WT HIV-RT. Some residues are omitted for clarity.

naphthyl azines **8c** and **8f** are particularly notable; they have sub-10 nM potency towards wild-type HIV-1 and viral variants containing the clinically important Y181C and K103N/Y181C mutations, greater activity than efavirenz particularly towards the K103N-bearing variant, normal cytotoxicity, and solubility, that is, ca. 1000-fold greater than for rilpivirine.

Acknowledgements

Gratitude is expressed to the National Institutes of Health (AI27690, AI44616, GM32136, GM49551) for research support and fellowship support for K. M. F. (AI104334). Receipt of reagents through the NIH AIDS Research and Reference Reagent Program, Division of AIDS, NIAID, NIH is also greatly appreciated. For beam-line access, we thank the National Synchrotron Light Source and the Northeastern Collaborative Access Team, which is funded by the NIH (P41 GM103403). This research used resources of the Advanced Photon Source, a U.S. Department of Energy facility at Argonne National Laboratory under Contract DE-AC02-06CH11357.

References and notes

1. Reynolds, C.; de Konig, C. B.; Pelly, S. C.; van Otterlo, W. A. L.; Bode, M. L. *Chem. Soc. Rev.* **2012**, *41*, 4657.
2. Permpalung, N.; Putcharoen, O.; Avihingsanon, A.; Ruxrungtham, K. *Exp. Opin. Pharmacother.* **2012**, *13*, 2301.
3. Kinch, M. S.; Patridge, E. *Drug Discovery Today* **2014**, *19*, 1510.
4. Margolis, A. M.; Heverling, H.; Pham, P. A.; Stolbach, A. J. *Med. Toxicol.* **2014**, *10*, 26.
5. Srinivasa, S.; Grinspoon, S. K. *Eur. J. Endocrinol.* **2014**, *170*, R185.
6. Bollini, M.; Domaoal, R. A.; Thakur, V. V.; Gallardo-Macias, R.; Spasov, K. A.; Anderson, K. S.; Jorgensen, W. L. *J. Med. Chem.* **2011**, *54*, 8582.
7. Lee, W.-G.; Gallardo-Macias, R.; Frey, K. M.; Spasov, K. A.; Bollini, M.; Anderson, K. S.; Jorgensen, W. L. *J. Am. Chem. Soc.* **2013**, *135*, 16705.
8. Lee, W.-G.; Frey, K. M.; Gallardo-Macias, R.; Spasov, K. A.; Bollini, M.; Anderson, K. S.; Jorgensen, W. L. *ACS Med. Chem. Lett.* **2014**, *5*, 1259.
9. Jorgensen, W. L.; Duffy, E. M. *Adv. Drug Deliv. Rev.* **2002**, *54*, 355.
10. Bollini, M.; Frey, K. M.; Cisneros, J. A.; Spasov, K. A.; Das, K.; Bauman, J. D.; Arnold, E.; Anderson, K. S.; Jorgensen, W. L. *Bioorg. Med. Chem. Lett.* **2013**, *23*, 5209.
11. Bollini, M.; Cisneros, J. A.; Spasov, K. A.; Anderson, K. S.; Jorgensen, W. L. *Bioorg. Med. Chem. Lett.* **2013**, *23*, 5213.
12. Baka, E.; Comer, J. E. A.; Takács-Novák, K. J. *Pharm. Biomed. Anal.* **2008**, *46*, 335.
13. Frey, K. M.; Puleo, D. E.; Spasov, K. A.; Bollini, M.; Jorgensen, W. L.; Anderson, K. S. *J. Med. Chem.* **2015**, *58*, 2737.
14. Recombinant RT52A enzyme was expressed, purified, and co-crystallized with 0.5 μ M rilpivirine in an optimized condition of 16–20% v/v PEG 8000, 50 mM HEPES (pH 7.0), 100 mM ammonium sulfate, 15 mM magnesium sulfate, and 5 mM spermine-HCl using hanging drop vaporization. Crystals were then transferred to a stabilizing solution containing 22% PEG 8000 and compounds **7g** and **8f** were soaked overnight (final concentration of 0.5 mM). Soaked crystals were then flash cooled in liquid nitrogen in a stabilizing solution containing 27% ethylene glycol. Diffraction data for the RT:**7g** complex was collected at NSLS on beam line X29A; data for RT:**8f** was collected at APS on beam line 24-ID-E through NE-CAT. Diffraction data for the RT:**7g** complex was processed using HKL2000; diffraction data for the RT:**8f** complex was processed using XDS. Phases were obtained using difference Fourier methods for the RT:**7g** complex or molecular replacement with Phaser for RT:**8f**. Structures were refined using Phenix until acceptable geometry and refinement statistics were achieved. Atomic coordinates and structure factors are deposited in the PDB with codes **5C24** (RT:**7g**) and **5C25** (RT:**8f**).
15. Janssen, P. A. J.; Lewi, P. J.; Arnold, E.; Daeyaert, F.; de Jonge, M.; Heeres, J.; Koymans, L.; Vinkers, M.; Guillemont, J.; Pasquier, E.; Kukla, M.; Ludovici, D.; Andries, K.; de Bethune, M.-P.; Pauwels, R.; Das, K.; Clark, A. D., Jr.; Frenkel, Y. V.; Hughes, S. H.; Medaer, B.; De Knaep, F.; Bohets, H.; De Clerck, F.; Lampo, A.; Williams, P.; Stoffels, P. J. *Med. Chem.* **1991**, *2005*, 48.